Fano resonances in electronic transport through a single-electron transistor

J. Göres,* D. Goldhaber-Gordon,† S. Heemeyer, and M. A. Kastner‡
Department of Physics, Massachusetts Institute of Technology, Cambridge, Massachusetts 02139

Hadas Shtrikman, D. Mahalu, and U. Meirav
Braun Center for Submicron Research, Weizmann Institute of Science, Rehovot, Israel 76100
(Received 27 December 1999; revised manuscript received 15 March 2000)

We have observed asymmetric Fano resonances in the conductance of a single-electron transistor resulting from interference between a resonant and a nonresonant path through the system. The resonant component shows all the features typical of single-electron addition to the confined droplet within the transistor, but the origin of the nonresonant path is unclear. A feature of this experimental system, compared to others that show Fano line shapes, is that changing the voltages on various gates allows one to alter the interference between the two paths.

I. INTRODUCTION

When a droplet of electrons is confined to a small region of space and coupled only weakly to its environment, the number of electrons and their energy become quantized. The analogy between such a system and an atom has proved to be quite close. In particular, these artificial atoms exhibit properties typical of natural atoms, including a charging energy for adding an extra electron and an excitation energy for promoting confined electrons to higher-lying energy levels.[1,2] Remarkably, the analogy goes even further and includes cases where an artificial atom interacts with its environment. A system known as a single-electron transistor (SET), in which an artificial atom is coupled to conducting leads, can be accurately described by the Anderson model.[3–5] The same model has been used extensively to study the interaction of localized electrons with delocalized ones within a metal containing magnetic impurities. One of its subtle predictions is the Kondo effect, which involves many-body correlations between an electronic spin on an impurity atom and those in the surrounding metal. This effect has recently been observed in a SET when the artificial atom develops a net spin because of an odd electron occupancy.[6–10] In this paper we report that by changing the parameters in a single-electron transistor we observe another phenomenon typical of natural atoms: Fano resonances. While several aspects of the Fano resonances in our SETs are easily understood, others are very surprising.

Asymmetric Fano line shapes are ubiquitous in resonant scattering,[11–13] and are observed whenever resonant and nonresonant scattering paths interfere. The more familiar symmetric Breit-Wigner or Lorentzian line shape[14] is a limiting case that occurs when there is no interference, for example when there is no nonresonant scattering channel. Fano resonances have been observed in a wide variety of experiments including atomic photoionization,[15] electron and neutron scattering,[16,17] Raman scattering,[18] and photoabsorption in quantum well structures.[19,20]

The widely successful application of the Landauer-Büttiker formalism[21,22] shows that electron transport through a mesoscopic system is closely analogous to scattering in the systems described above. Therefore, one might expect to also observe Fano resonances in the conductance of nanostructures.[23–26] Indeed, Fano line shapes have been reported in a recent experiment by Madhavan *et al.* measuring tunneling from a scanning tunnel microscope tip through an impurity atom into a metal surface.[27] However, this characteristic feature of interference between resonant and nonresonant scattering has not been reported for more conventional nanostructures.

In this paper we report the observation of Fano resonances in conductance through a SET. This system has the advantage over the tunneling experiment of Madhavan *et al.*[27] and over conventional scattering experiments in that we can tune the key parameters and thus study the interference leading to Fano resonances in greater detail. This paper is organized as follows: In Sec. II we describe the SET and the measurements we have made on it; we also summarize the standard theory for Fano line shapes. Our results are presented in Sec. III. In Sec. IV we discuss the results, draw conclusions and point out issues that require further research.

II. EXPERIMENTAL DETAILS AND THEORETICAL BACKGROUND

A SET consists of a small droplet of electrons coupled to two conducting leads by tunnel barriers. Gate electrodes (shown in Fig. 1) are used to control the electrostatic potential of the droplet and, in our structures, the heights of the tunnel barriers. The SETs used in these experiments are the same ones used for studies by Goldhaber-Gordon *et al.* of the Kondo effect.[6,7] The electron droplet is created in a two-dimensional electron gas (2DEG) that forms at the interface of a GaAs/AlGaAs heterostructure with a mobility of $100\,000\ \mathrm{cm}^2/\mathrm{Vs}$ and a density of $8.1\times10^{11}\ \mathrm{cm}^{-2}$. Applying a negative voltage to two pairs of split gate electrodes depletes the 2DEG underneath them and forms two tunnel barriers. The barriers separate the droplet of electrons from the 2DEG regions on either side, which act as the leads. The heights of the two barriers can be adjusted independently by changing the voltages on the respective constriction electrodes (I), and the potential energy of the electrons on the

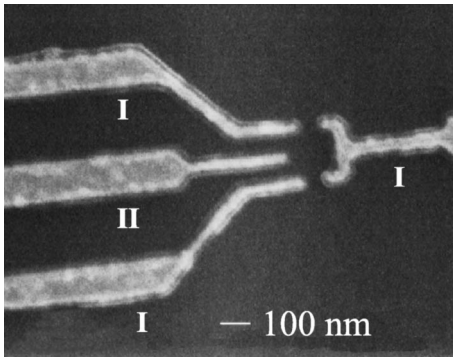

FIG. 1. Electron micrograph of a SET showing the split gates (*I*) that define the tunnel barriers and the additional gate electrode (*II*) that adjusts the potential energy on the droplet.

droplet can be shifted relative to the Fermi energies in the leads using an additional plunger gate electrode (*II*) near the droplet.

Our SETs are made with a 2DEG that is closer to the surface (≈ 20 nm) than in most other experiments, allowing the electron droplet to be confined to smaller dimensions. This also makes the tunnel barriers more abrupt than in previous structures. We estimate that our droplet is about 100 nm in diameter, smaller than the lithographic dimensions because of depletion, and contains about 50 electrons.

For conductance measurements we apply a small alternating drain-source voltage (typically 5 μV) between the leads and measure the preamplified current with a lock-in amplifier. The conductance is then recorded as a function of the plunger gate voltage V_g. For differential conductance measurements we add a finite offset drain-source voltage V_{ds} and measure the response dI/dV_{ds} to the small alternating drain-source voltage as a function of both V_g and V_{ds}.

In a SET the Coulomb interaction among electrons opens up an energy gap U in the tunneling spectrum, given classically by $e^2/2C$, where C is the total capacitance between the the droplet and its environment, primarily the nearby conducting leads and gates. Thus, an energy U is required to overcome Coulomb repulsion and add an electron to the droplet. This energy cost causes the number of electrons on the droplet to be quantized and electron transport through the droplet to be suppressed. However, lowering the electrochemical potential of the droplet by adjusting the voltage on the plunger gate makes it possible to add electrons one at a time. At a charge degeneracy point, where the states with N and $N+1$ electrons on the droplet have equal energy, transport of electrons from one lead through the droplet to the other lead is allowed. This effect is known as Coulomb blockade[28] because transport is suppressed everywhere except close to the degeneracy points. Because of the small size of the electron droplet in our SETs, the energy spacing between the discrete levels $\Delta\epsilon$, that is, the energy to excite the droplet at fixed N, is only a few times smaller than the charging energy U.

Depending on the transmission of the left and right tunnel barriers, characterized by tunneling rates $\Gamma_L/h, \Gamma_R/h$, respectively, we observe different transport regimes in our SETs at low temperature. Each time we cool a particular SET to low temperatures we find different tunneling rates of the barriers and a different electrochemical potential of the electron droplet, for the same electrode voltages. This probably reflects the metastability, at low temperature, of electrons in the donor layer within the AlGaAs. Also possibly related to this metastability are events in which the effective voltage of a particular electrode suddenly changes to a different value. We suspect that this results from charge motion around an impurity or a defect near the artificial atom. As much as possible, we have avoided using measurements in which such events occur.

If the thermal energy k_BT is much smaller than the coupling energy $\Gamma \equiv \Gamma_L + \Gamma_R$, quantum fluctuations dominate so that the resonances have width Γ. When $\Gamma \ll \Delta\epsilon$, the coupling is weak and one observes narrow quasiperiodic peaks [Fig. 2(c)] at accessible temperatures. When the coupling is larger a new regime emerges, in which transport between pairs of resonances is enhanced by the Kondo effect[6] if there is an odd number of electrons on the droplet [Fig. 2(b)]. Surprisingly, when the coupling is still larger we observe asymmetric Fano resonances on top of a slowly varying background [Fig. 2(a)].

Note that the Fano regime in Fig. 2 has been obtained in a different cool down from the other two regimes, but we have observed each of these three types of behavior many times for several samples. Although we cannot continuously tune between the different regimes of Fig. 2, and although the maximum conductance is lower in Fig. 2(a) than in Fig. 2(b), the much larger background conductance leads us to believe that the tunnel couplings are increased compared to the Kondo regime. Because of differences in the electrochemical potential of the droplet in each cool down, the absolute values of the electrode voltages in the different regimes cannot be directly compared. Nonetheless, as discussed below, we use the drain-source voltage dependence and the temperature dependence to determine the important energy scales in each regime. In particular, the scale factor between plunger gate voltage and electrochemical potential of the electron droplet does not change appreciably for the three data sets shown in Fig. 2.

Before discussing the data in detail, we review the analytic form predicted for Fano line shapes. Scattering (*S* matrix) theory predicts Fano line shapes as the general form for resonances in transport through quasi-1D systems.[23] The resonant amplitude has a phase shift that varies from zero to π as the energy is moved through the resonance from below. That is, the resonant contribution to the phase shift $\delta_{res}(\epsilon)$ is given by $\tan\delta_{res}(\epsilon) = -\Gamma/2(\epsilon - \epsilon_0)$. On the other hand, any background or nonresonant contribution to the scattering phase shift δ_0 is slowly varying and is assumed to be independent of the energy. The total cross section is directly related to the scattering phase shifts through

$$\sigma(\epsilon) \propto \sin^2[\delta_{res}(\epsilon) + \delta_0]. \tag{1}$$

Varying the value of the background phase shift produces the entire family of Fano line shapes.

It is important to emphasize that two interfering channels are necessary for Fano resonances to arise. One is resonant, for which the phase changes by π in an energy interval $\approx\Gamma$ around the resonance energy ϵ_0. The other is nonresonant and has a constant background phase shift δ_0. If there is no nonresonant channel or the background phase shift between

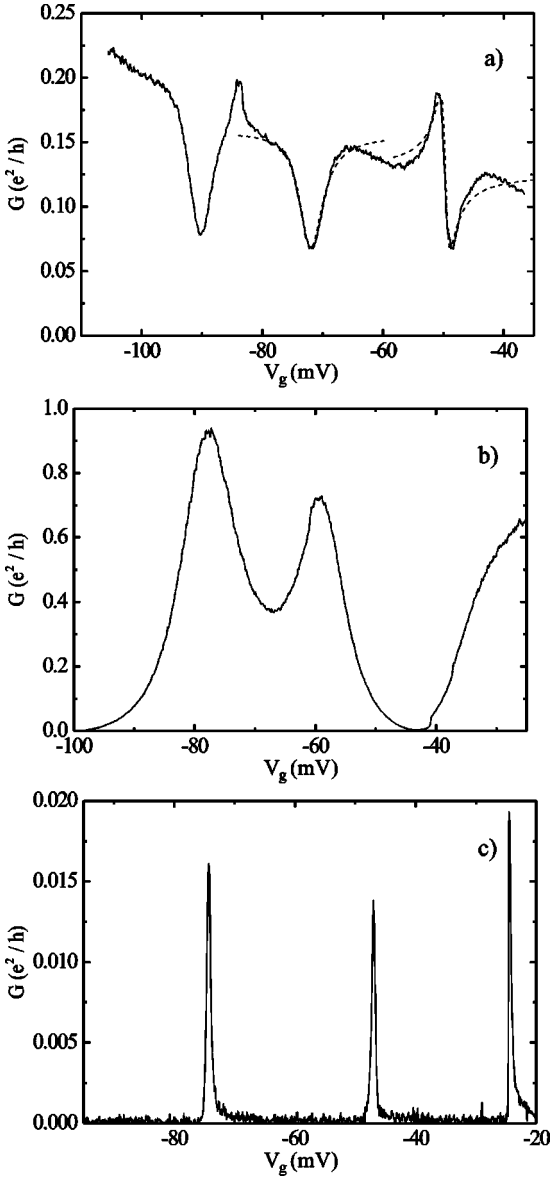

FIG. 2. Comparison of conductance measurements in the (a) Fano regime, (b) Kondo regime (Ref. 6), and (c) weak-coupling regime (Ref. 6). From (c) to (b) to (a) the coupling between the droplet and the leads increases (see the text). Fits to the Fano formula Eq. (3) are shown for the center and right resonances in (a). The respective asymmetry parameters are $q=-0.03$ and $q=-0.99$. During the sweep through the left resonance a sudden shift in effective plunger gate voltage occured, presumably caused by charge motion in the vicinity of the droplet, leading to the unusual shape of this resonance.

the channels is zero, symmetric Breit-Wigner resonances are observed. In all other cases Fano resonances result.

In his original work Fano treated the case of inelastic scattering in the context of autoionization and derived the so-called Fano formula for the scattering cross section[11]

$$\sigma(\epsilon)\propto\frac{(\tilde{\epsilon}+q)^2}{\tilde{\epsilon}^{\,2}+1}, \tag{2}$$

where $\tilde{\epsilon}\equiv(\epsilon-\epsilon_0)/(\Gamma/2)$ is the dimensionless detuning from resonance and q is called the asymmetry parameter. The asymmetry parameter is related to the background phase shift of the S-matrix treatment by $q=\cot\delta_0$. The magnitude of q is proportional to the ratio of transmission amplitudes for the resonant and nonresonant channels.[11] The limit $q\rightarrow\infty$, in which resonant transmission dominates, leads to symmetric Breit-Wigner resonances. In the opposite limit $q\rightarrow 0$ nonresonant transmission dominates, resulting in symmetric dips.

According to the Landauer-Büttiker formalism, conductance through any mesoscopic system can be expressed in terms of an S matrix. Hence, Fano resonances should also be observed in conductance if resonant and a nonresonant transmission paths coexist.[23] In analogy to the scattering case Eq. (2) the conductance is then given by

$$G=G_{\rm inc}+G_0\frac{(\tilde{\epsilon}+q)^2}{\tilde{\epsilon}^{\,2}+1}, \tag{3}$$

where $G_{\rm inc}$ denotes an incoherent contribution to the conductance, which is often observed.[29] Note that the Breit-Wigner limit $q\rightarrow\infty$ implies $G_0\rightarrow 0$ leading to a finite conductance maximum of $G_{\rm inc}+G_0(1+q^2)$ at $\tilde{\epsilon}=1/q$.

III. RESULTS

As mentioned above, Fig. 2(a) shows three consecutive, well-separated and relatively narrow resonances on a background that varies smoothly in the range 0.11–0.22 e^2/h. The conductance does not vanish at resonance, as would occur if the destructive interference between the transmission paths were complete, presumably because an incoherent component is present. The resonances in the center and right are of the Fano form Eq. (3) with asymmetry parameters given in the figure caption.

We might imagine that we could calculate the combined transmission through the resonant and nonresonant channels simply by adding the complex amplitudes for transmission through the two channels, each considered individually. In fact, the phase difference between the two transmissions, and hence the degree of asymmetry of the resonant line shape, depends on the relative strengths of transmission through the two channels. This means that just by changing the *strength* of resonant transmission we can change the shape of the Fano profile in a way that would naively seem to require changes in *phase* of one or both transmissions. This effect can be achieved experimentally by varying the voltages on our point-contact electrodes, thereby changing the strength of transmission through each of the two channels, and generally changing the ratio of their strengths as well.

A separate cool down has been made to explore the influence of the strength of the tunnel couplings $\Gamma_{\rm L}$ and $\Gamma_{\rm R}$ on the resonances, and the results are shown in Fig. 3. All the resonances in this figure can be fit very well by the Fano formula [Eq. (3)]. The fitting parameters for the data in Figs. 3(a) and 3(b) are plotted in Figs. 3(c) and 3(d), respectively. Increasing $\Gamma_{\rm L}$ leads to a more symmetric line shape, while the difference between maximum and minimum conductance remains approximately constant. This is reflected in a strong increase of the asymmetry parameter q accompanied by a decrease in G_0 leaving the product $G_0(1+q^2)$ nearly unchanged. The decrease in magnitude of the negative voltage

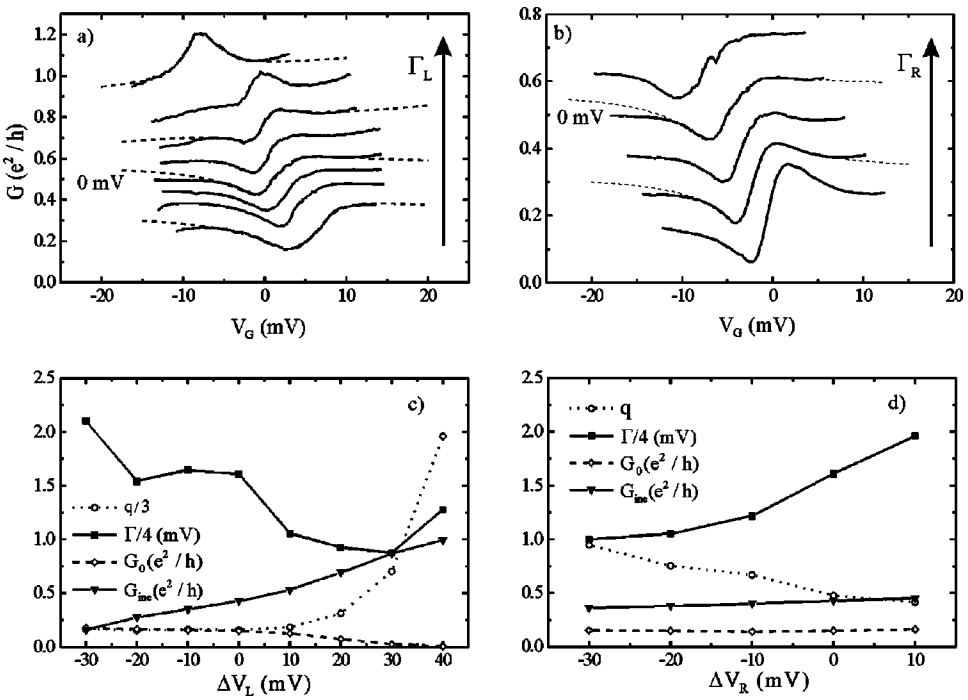

FIG. 3. Conductance resonances as a function of the plunger gate voltage for various strengths of the tunnel couplings (a) Γ_L and (b) Γ_R. The data sets labeled 0 mV are identical for both (a) and (b) and correspond to the case where -145 mV is applied to both the left and the right split gate electrodes (labeled *I* in Fig. 1). The couplings are increased in the direction of the arrows by successively increasing the voltages on the respective electrodes in 10 mV steps. All resonances are displaced horizontally to account for the capacitative shifts of the resonance positions caused by the different applied plunger gate voltages. The resonances in (b) are displaced vertically for clarity in 0.1 e^2/h steps. This was not necessary in (a) because of the substantial variation of the background. The dashed curves are obtained by fitting the Fano formula Eq. (3) to the resonances. The best-fitting parameters for the resonances in (a) and (b) are given in (c) and (d), respectively. The parameter Γ is given in mV of plunger gate voltage. Multiplication by $\alpha \approx 0.06$ converts these into energy units (meV).

on the left constriction electrodes [Fig. 3(a)] also causes the incoherent background to increase substantially. In addition, a slight decrease in Γ is observed. By contrast, increasing Γ_R leaves the magnitude of the incoherent transmission constant and decreases the asymmetry parameter. At the same time the resonance is broadened, as reflected by an increase in Γ.

To clarify the origin of the resonant and nonresonant components of the conductance we next examine the temperature and drain-source voltage dependencies of the Fano line shapes. In a different cooldown from those of Figs. 2 and 3 we have found consecutive Fano resonances with small asymmetry parameters, resulting in nearly symmetric dips; these are shown for a variety of temperatures in Fig. 4(a). The increase in width of the resonances with increasing temperature is in good agreement with the linear $3.5k_BT$ dependence expected from Fermi-Dirac broadening [Fig. 4(c)]. From this we obtain the conversion factor $\alpha = 0.059 \pm 0.006$ that relates plunger gate voltage to electrochemical potential by $eV_g = \alpha\mu$. As mentioned above, this is in reasonable agreement with values found for the other regimes in Fig. 2.

In contrast to the width dependence, the temperature dependence of the dip amplitude is not that expected from Fermi-Dirac broadening but rather is reminiscent of that seen for peaks in the Kondo regime.[7] Indeed, the amplitude, measured with respect to the background, shows a logarithmic dependence on T over almost an order of magnitude as shown in Fig. 4(b). In addition, the symmetric dip on the right shows a shift of the resonance energy with temperature suggesting that the energy is renormalized at low temperatures just as for conductance peaks in the Kondo regime. These data resemble curves obtained from a mean-field treatment of quantum interference in the Kondo regime.[30]

The situation becomes even more intriguing when one examines the differential conductance as a function of both plunger gate voltage and drain-source voltage. The two resonances in Fig. 4 are accompanied by a third near $V_g = -150$ mV. Unfortunately, switching events have made it difficult for us to study the temperature and drain-source voltage dependencies of all three resonances, even though we have measured both dependencies in the same cooldown. We show the differential conductance for the two peaks near $V_g = -110$ and -150 mV on a gray-scale plot in Fig. 5, where a clear diamond-shaped structure is traced out by the resonances as one varies the two voltages. This behavior is familiar from many experiments in the Coulomb blockade regime.[31–33] Indeed, close scrutiny reveals additional dips moving parallel to those forming the main diamonds, analogous to subsidiary peaks seen in the Coulomb blockade regime, which result from excited states of the electron droplet.

However, the results in Fig. 5 are different in important ways. The resonances are dips rather than peaks, and they appear on top of a continuous background conductance that is almost independent of the applied voltages.

From the slopes of the diamonds' boundaries it is possible to determine the parameters $\alpha = C_{\text{gate}}/C_{\text{tot}} = 0.049 \pm 0.005$ and $\beta = C_{\text{lead}}/C_{\text{tot}} = 0.66 \pm 0.09$. Here C_{tot} is the total capacitance coupling the electron droplet to its environment, whereas C_{gate} is the capacitance only to the plunger gate, and

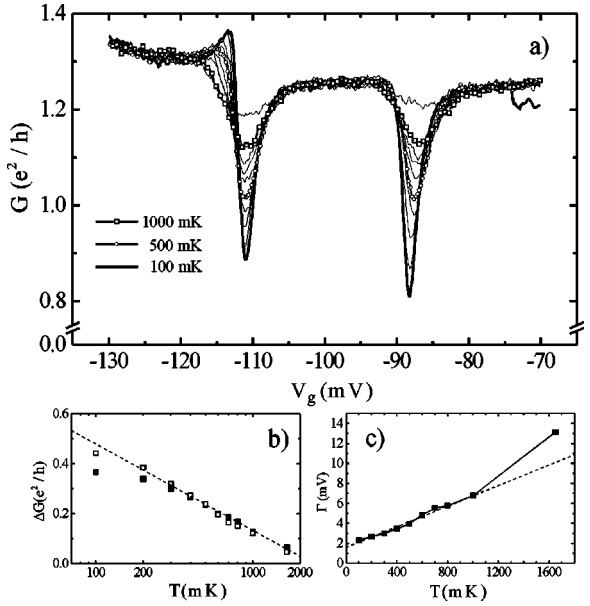

FIG. 4. (a) Temperature dependence of the conductance for two resonances. At 100 mK the asymmetry parameters for the left and right resonances are $q=-0.35$ and $q=-0.13$, respectively. The background has been adjusted for a slight increase with temperature, corresponding to only 0.06 e^2/h at the highest temperatures. (b) Dip amplitude with respect to the background conductance as a function of temperature. (c) Width Γ, measured in mV of plunger gate voltage, of the right resonance as a function of temperature as determined from a fit to the Fano formula [Eq. (3)]. The slope of the linear fit (dashed line) at low temperatures gives a value of $\alpha=0.059\pm0.006$ relating plunger gate voltage to energy.

C_{lead} the capacitance only to one of the leads. The value for α is in good agreement with the one obtained from the temperature dependence above.

The bottom resonance in Fig. 5 near $V_g=-115$ mV is identical to the left one in Fig. 4 allowing us to determine the two spacings in plunger gate voltage for three successive peaks. Based on the constant-interaction model[1] we assume

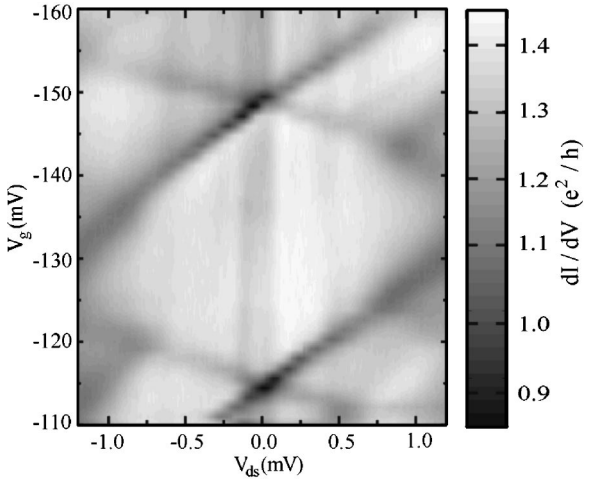

FIG. 5. Differential conductance (dI/dV_{ds}) at $T=100$ mK as a function of both the bias voltage V_{ds} across the SET and the plunger gate voltage V_g. Notice that the features are produced by dips in the conductance rather than peaks and that there are weak features near $V_{\text{ds}}=0$.

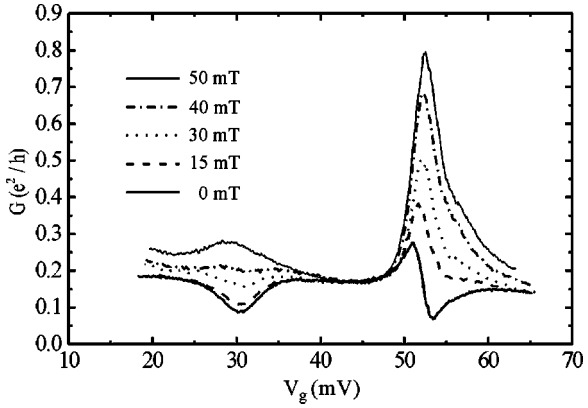

FIG. 6. Conductance as a function of plunger gate voltage for various magnetic fields applied perpendicular to the 2DEG.

that the smaller spacing is given by U/α and the larger by $(U+\Delta\epsilon)/\alpha$. Using this and the width from Fig. 4, we find $U=1.13\pm0.12$ meV, $\Gamma=105$–120 μeV, and $\Delta\epsilon=0.66\pm0.07$ meV. It is surprising that the charging energy is only about 40% smaller than Goldhaber-Gordon *et al.* report in the Kondo regime[7] for the same device in a separate cool down. One expects the Coulomb charging energy to decrease as the tunnel barriers are lowered.[31] It is even more surprising that Γ has decreased by 50% compared to the Kondo regime,[7] rather than increasing as expected, even though we have opened up the tunnel barriers resulting in a sizable nonresonant conductance and resonant dips instead of peaks.

Reminiscent of the Kondo regime are features that remain pinned near $V_{\text{ds}}=0$ as the plunger gate voltage is varied, seen as a faint vertical stripe in the center of Fig. 5. In the Kondo regime this results from a sharp peak in the density-of-states at the Fermi energy caused by coupling of the localized spin on the artificial atom to the spins in the metallic leads. However, in Fig. 5 the features do not depend on whether an even or odd number of electrons is on the droplet as evinced by their spanning more than two resonances. Furthermore, the zero-bias peak in the measurements of Goldhaber-Gordon *et al.*[7] has an amplitude that depends strongly on the separation in V_g from the resonance, whereas the features in Fig. 5 are nearly independent of V_g.

The effect of a magnetic field perpendicular to the 2DEG containing the electron droplet is dramatic (Fig. 6). This measurement has been made in a separate cool down. A field of only 15 mT produces a clear effect on the line shape, and a field of 50 mT completely transforms the left-hand resonance from an asymmetric one with a dip into an asymmetric peak.

IV. DISCUSSION

A. Nature of interfering channels

The good fit of the Fano form to our measurements makes it clear that we are observing interference between resonant and nonresonant paths through our SET. Were electrons noninteracting, it would not be surprising for resonant and nonresonant transmission to coexist. We can see this with the help of a semiclassical noninteracting analog for the SET: a cavity with two small openings to reservoirs on the left and right sides. Electrons incident on the cavity from the left side

at a random angle would bounce around the cavity, only achieving significant transmission to the right should their energy match an eigenenergy of the cavity. This process would give resonant transmission. In contrast, electrons incident on the left side at exactly the correct angle could traverse the cavity and leave through the righthand opening without suffering any bounces inside the cavity. This is a nonresonant process, independent of electron energy.

However, in our case the resonant channel shows all the features typical of charging of artificial atoms: the near periodicity in plunger gate voltage of the conductance resonances and the diamond structure and additional features associated with excited states in the differential conductance. It is surprising that we see such strong evidence for charge quantization (Fig. 5) coexisting with a continuous open channel through our SET.

We can resolve this apparent contradiction if two paths for an electron through the SET have traversal times long and short, respectively, compared to $\hbar/U$. The path that spends a long time in the region of the electron droplet (passing through a well-localized state) must respect the charging energy, so it exhibits Coulomb blockade resonances in conductance. The other path can temporarily violate energy conservation, adding a charge to the electron droplet during a rapid traversal of the SET.[34] Based on a suggestion by Brouwer,[35] we have calculated the time required for ballistic traversal of our electron droplet across the confined region and find it to be comparable to $\hbar/U$.

A puzzle remains: How can the resonances be quite narrow [Fig. 4(a)] even though the point contacts are more open than in the Kondo regime [Fig. 2(b)], as demonstrated by a nonresonant background conductance larger than e^2/h? Conductance through a point contact in the lowest subband cannot exceed $2e^2/h$, corresponding to a transmission probability of unity. When electrons can be transmitted across a point contact into two distinct states, the *sum* of the two transmissions can be no greater than unity. So a large transmission across the first point contact into the delocalized state that ballistically traverses the electron droplet, implies a correspondingly reduced transmission into the localized, resonant state. The same analysis holds for electrons traversing the second point contact to exit the droplet. The width Γ of a resonant state is given by the rate of escape of electrons from that state, which is in turn proportional to the sum of the transmissions across the two point contacts into or out of that state. This explains how the presence of a nonresonant transmission channel can actually make the transmission resonances sharper.[36]

We have considered alternative explanations for the origin of the nonresonant background conductance and find them unlikely. A path that circumvents the electron droplet might lead to a continous contribution to the conductance. However, a parallel conduction path in the dopant layer above the 2DEG has been ruled out by Hall and Shubnikov-de Haas measurements on samples from the same wafer with large-area gate electrodes. Since we observe Fano resonances in each of several devices we have studied, it also seems unlikely that the effect is a consequence of channels bypassing the quantum dot in the plane of the 2DEG, caused by lithographic defects or nonuniform charge distributions. Most importantly, should a path circumvent the electron droplet the resulting background would be incoherent. For interference it is important that both paths include the two point contacts since only they can act as coherent source and detector.

Detailed measurements of the evolution from the Kondo regime to the Fano regime are underway, with the hope of further elucidating the nature of the nonresonant background conductance.

B. Magnetic-field dependence

Changes in transport even at very small field scales are not unexpected given the droplet's geometry and the 2DEG properties. For our nonresonant transmission, electrons traverse the droplet directly, so backscattered paths enclose approximately the area of the droplet. Assuming an electron droplet of 100 nm diameter, one flux quantum $\Phi_0 \equiv h/e$ penetrates the droplet at approximately 530 mT applied field. Thus, at this field scale, changes in nonresonant conductance would result from the breakdown of coherent backscattering.[37] However, the resonant path through our droplet is less strongly connected to the leads, so electrons traverse the droplet by more roundabout paths, enclosing more net area than simply that of the droplet. This means that breakdown of coherent backscattering should occur at much lower flux through the droplet, $\Phi_{\mathrm{corr}} = \Phi_0 / \sqrt{g(\Delta\epsilon/\Gamma)}$, where $g \equiv G/(2e^2/h)$ is the dimensionless conductance of the droplet itself.[37] We saw earlier that $\Delta\epsilon/\Gamma \approx 5$; and g should be comparable to the conductance of the 2DEG $g_{2D} \approx 300$, though somewhat suppressed because the electron density of the droplet is less than that of the 2DEG.[38] Taking $g = g_{2D}$, we arrive at 12 mT as an estimate and lower bound for Φ_{corr}, consistent with our empirical observations.[39]

Empirically (Fig. 6), small magnetic fields produce dramatic alterations in the resonances, while leaving the nonresonant background essentially unchanged. The argument made above explains the changes in transport at small magnetic fields as resulting from the breakdown of coherent backscattering in the resonant channel, and the concomitant increase in forward transmission through that channel. Since nonresonant transmission is not affected at these low fields, the net result is an enhancement of q. The alternative explanation—that the magnetic field destroys the interference between nonresonant and resonant processes, transforming resonant dips into peaks—does not account for the extremely low-field scale at which the change occurs, nor does it fully match the data. The breakdown of coherent backscattering indeed is caused by the loss of the special phase relation between pairs of *time-reversed* paths, but here we are concerned with interference between two distinct *forward-scattering* paths (resonant and nonresonant) which do not form a time-reversed pair. In addition, interpreting the zero-field data as the simple interference between two paths would suggest that the resonant path has half the amplitude of the nonresonant path. Yet applying a field causes the resonant contribution of the right-hand peak to exceed the nonresonant background by a factor of 3. Both these considerations lead us to believe that changes in amplitude (and perhaps phase) for the resonant process due to applied field are more important than destruction of coherence by that field.

ACKNOWLEDGMENTS

We acknowledge fruitful discussions with P. Brouwer, L. I. Glazman, R. J. Gordon, G. Schön, H. Schöller, S. H. Simon, A. Yacoby, and especially J. U. Nöckel and Ned Wingreen. J. G. thanks NEC, and D. G.-G. thanks the Hertz Foundation for financial support. This work was supported by the US Army Research Office under Contract No. DAAG 55-98-1-0138, and by the National Science Foundation under Grant No. DMR-9732579.

*Present address: Max-Planck-Institut für Festkörperforschung, Heisenbergstraße 1, 70569 Stuttgart, Germany.

†Present address: Harvard University, Department of Physics and Society of Fellows, 17 Oxford Street, Cambridge MA 02138.

‡Electronic address: mkastner@mit.edu

[1] M.A. Kastner, Phys. Today **46**, 24 (1993).

[2] R.C. Ashoori, Nature (London) **379**, 413 (1996).

[3] T.K. Ng and P.A. Lee, Phys. Rev. Lett. **61**, 1768 (1988).

[4] L.I. Glazman and M.E. Raikh, Pis'ma Zh. Éksp. Teor. Fiz. **47**, 378 (1988) [JETP Lett. **47**, 452 (1988)].

[5] Y. Meir, N.S. Wingreen, and P.A. Lee, Phys. Rev. Lett. **70**, 2601 (1993).

[6] D. Goldhaber-Gordon, H. Shtrikman, D. Mahalu, D. Abusch-Magder, U. Meirav, and M.A. Kastner, Nature (London) **391**, 156 (1998).

[7] D. Goldhaber-Gordon, J. Göres, M.A. Kastner, H. Shtrikman, D. Mahalu, and U. Meirav, Phys. Rev. Lett. **81**, 5225 (1998).

[8] S.M. Cronenwett, T.H. Oosterkamp, and L.P. Kouwenhoven, Science **281**, 540 (1998).

[9] J. Schmid, J. Weis, K. Eberl, and K.v. Klitzing, Physica B **256-258**, 182 (1998).

[10] F. Simmel, R.H. Blick, J.P. Kotthaus, W. Wegscheider, and M. Bichler, Phys. Rev. Lett. **83**, 804 (1999).

[11] U. Fano, Phys. Rev. **124**, 1866 (1961).

[12] H. Feshbach, D.C. Peaslee, and V.F. Weisskopf, Phys. Rev. **71**, 145 (1947).

[13] A. Shibatani and Y. Toyozawa, J. Phys. Soc. Jpn. **25**, 335 (1968).

[14] G. Breit and E. Wigner, Phys. Rev. **49**, 519 (1936).

[15] U. Fano and J.W. Cooper, Phys. Rev. A **137**, 1364 (1965).

[16] R.K. Adair, C.K. Bockelman, and R.E. Peterson, Phys. Rev. **76**, 308 (1949).

[17] J.A. Simpson and U. Fano, Phys. Rev. Lett. **11**, 158 (1963).

[18] F. Cerdeira, T.A. Fjeldly, and M. Cardona, Phys. Rev. B **8**, 4734 (1973).

[19] J. Feist, F. Capasso, C. Sirtori, K.W. West, and L.N. Pfeiffer, Nature (London) **390**, 589 (1997).

[20] H. Schmidt, K.L. Campman, A.C. Gossard, and A. Imamoglu, Appl. Phys. Lett. **70**, 3455 (1997).

[21] R. Landauer, Z. Phys. B **68**, 217 (1987).

[22] M. Büttiker, IBM J. Res. Dev. **32**, 63 (1988).

[23] J.U. Nöckel and A.D. Stone, Phys. Rev. B **50**, 17 415 (1994).

[24] W. Porod, Z. Shao, and C.S. Lent, Appl. Phys. Lett. **61**, 1350 (1992).

[25] E. Tekman and P. Bagwell, Phys. Rev. B **48**, 2553 (1993).

[26] P.J. Price, Superlattices Microstruct. **20**, 253 (1996).

[27] V. Madhavan, W. Chen, T. Jamneala, M.F. Crommie, and N.S. Wingreen, Science **280**, 567 (1998).

[28] T.A. Fulton and G.J. Dolan, Phys. Rev. Lett. **59**, 109 (1987).

[29] The incoherent background G_{inc} is introduced to account for the nonvanishing conductance at the resonance minimum. We can also account for this behavior by assuming a complex asymmetry parameter q (Refs. 23 and 30).

[30] S. Heemeyer and X.-G. Wen (to be published).

[31] E.B. Foxman, P.L. McEuen, U. Meirav, N.S. Wingreen, Y. Meir, P.A. Belk, N.R. Belk, M.A. Kastner, and S.J. Wind, Phys. Rev. B **47**, 10 020 (1993).

[32] L.P. Kouwenhoven, T.H. Oosterkamp, M.W.S. Danoesastro, M. Eto, D.G. Austing, T. Honda, and S. Tarucha, Science **278**, 1788 (1997).

[33] J. Weis, R.J. Haug, K.v. Klitzing, and K. Ploog, Phys. Rev. Lett. **71**, 4019 (1993).

[34] This mechanism is an extension of the well-known cotunneling process that accounts for Lorentzian tails of Coulomb blockade conductance peaks.

[35] P. Brouwer (private communication). Since both sides of the inequality vary linearly with droplet radius, its validity does not depend on droplet radius, but it does require high Fermi velocity and hence high-electron density.

[36] It is also conceivable that the resonant and nonresonant transmissions could originate from separate lateral subbands of the point contacts. D.G. Baksheyev, O.A. Tkachenko, and V.A. Tkachenko, Physica E (Amsterdam) **6**, 414 (2000).

[37] R.A. Serota, Shechao Feng, C. Kane, and P.A. Lee, Phys. Rev. B **36**, 5031 (1987).

[38] H. van Houten, C.W.J. Beenakker, and A.A.M. Staring, *Single Charge Tunneling. Coulomb Blockade Phenomena in Nanostructures*, Proceedings of a NATO Advanced Study Institute, edited by H. Grabert and M.H. Devoret (Plenum, London, 1992), pp. 167–216.

[39] Reference 40 presents and Ref. 41 experimentally corroborates a result for Φ_{corr} slightly different from that derived in Ref. 37. Our experiment cannot distinguish between the two theoretical predictions, which differ by less than a factor of 2 for our parameters.

[40] I.L. Aleiner and L.I. Glazman, Phys. Rev. Lett. **77**, 2057 (1996).

[41] S.M. Cronenwett, S.R. Patel, C.M. Marcus, K. Campman, and A.C. Gossard, Phys. Rev. Lett. **79**, 2312 (1997).